Soft Matter

PAPER

View Article Online
View Journal | View Issue

Cite this: *Soft Matter*, 2015, **11**, 4326

Phase behavior of skin lipid mixtures: the effect of cholesterol on lipid organization†

E. H. Mojumdar, G. S. Gooris and J. A. Bouwstra*

Received 15th December 2014,
Accepted 28th April 2015

DOI: 10.1039/c4sm02786h

www.rsc.org/softmatter

The lipid matrix in the *stratum corneum* (SC), the upper layer of the skin, plays a critical role in the skin barrier. The matrix consists of ceramides (CERs), cholesterol (CHOL) and free fatty acids (FFAs). In human SC, these lipids form two coexisting crystalline lamellar phases with periodicities of approximately 6 and 13 nm. In the studies reported here, we investigated the effect of CHOL on lipid organization in each of these lamellar phases separately. For this purpose, we used lipid model mixtures. Our studies revealed that CHOL is imperative for the formation of each of the lamellar phases. At low CHOL levels, the formation of the lamellar phases was dramatically changed: a minimum 0.2 CHOL level in the CER/CHOL/FFA (1 : 0.2 : 1) mixture is required for the formation of each of the lamellar phases. Furthermore, CHOL enhances the formation of the highly dense orthorhombic lateral packing. The gradual increment of CHOL increases the fraction of lipids forming the very dense orthorhombic lateral packing. Therefore, these studies demonstrate that CHOL is an indispensable component of the SC lipid matrix and is of fundamental importance for appropriate dense lipid organization and thus important for the skin barrier function.

1. Introduction

The skin barrier is crucial for terrestrial life. It protects the body from the environment and prevents the excessive transepidermal water loss.[1] This extraordinary function of the skin is provided by the outermost non-viable layer of the skin known as the *stratum corneum* (SC). The SC of human skin is about 15–20 μm thick and consists of dead flattened protein-filled cells referred to as corneocytes wrapped with a cornified envelope, a densely cross-linked protein layer with covalently attached lipids, referred to as bound lipids. In between the corneocytes a highly organized lipid matrix is present. As partitioning of compounds into the corneocytes is strongly reduced by the cornified envelope and the bound lipids, the lipid matrix acts as an important pathway for compounds penetrating through the SC.[2,3]

The main lipid classes in the SC are ceramides (CERs), cholesterol (CHOL) and free fatty acids (FFAs) in an approximately equimolar ratio.[4–8] Together these lipids can form two coexisting crystalline lamellar phases; the long periodicity phase (LPP) with a repeat distance of approximately 13 nm and the short periodicity phase (SPP) with a repeat distance of approximately 6 nm.[9,10] Within the lipid lamellae, the lipids can be arranged in different structures that have different densities known as the lipid lateral packing. Depending on the lipid composition, the lateral packing can be either orthorhombic, hexagonal or liquid. At physiological skin surface temperature (~32 °C), the lipids in human SC preferably adopt an orthorhombic packing while a small population of lipids also assembles in a hexagonal packing.[9,11–14] Both the lamellar phases and the lateral packing are important and have shown to play a crucial role in maintaining a proper skin lipid barrier function.[15–18]

In our present study, we aimed to investigate the influence of CHOL on the lipid organization using lipid model mixtures. The significance of CHOL on the skin barrier has been studied and it has been reported that CHOL is required for building a proper lipid organization in SC and subsequently for a proper skin barrier function.[19–21] In phospholipid bilayers, it has been reported that CHOL plays a crucial role in maintaining the structure, fluidity and orientation of the lipids. It has also been reported that CHOL has a much higher affinity for saturated lipids compared to unsaturated ones.[22–24]

In previous studies it has been suggested that CERs are the key components and play an important role in the skin lipid barrier.[25] So far 14 different subclasses of CERs have been identified in human SC.[26,27] Four of these CER subclasses have an exceptionally long ω-hydroxy fatty acid chain ester linked to linoleic acid, referred to as CER EO. It has been reported that diminution of the level of CER EOS or complete abduction of CER EO leads to a reduction or even the absence of the LPP and thereby reduces the skin barrier function.[15,28–30] When focusing

Leiden Academic Center for Drug Research, Department of Drug Delivery Technology, Gorlaeus Laboratories, University of Leiden, Einsteinweg 55, 2333 CC Leiden, The Netherlands. E-mail: bouwstra@chem.leidenuniv.nl; Fax: +31 71 527 4565; Tel: +31 71 527 4208

† Electronic supplementary information (ESI) available. See DOI: 10.1039/c4sm02786h

on the FFAs, in the native human SC, most FFAs are saturated with a chain length distribution ranging from C14 to C34 with an average chain length between C20 and C22.[29,31] The importance of FFAs has also been reported in previous studies as these lipids enhance the formation of the orthorhombic lateral packing.[32,33]

There are not many studies published aiming to investigate the effect of CHOL on the SC lipid organization systematically.[34] A few studies report on the phase behavior of CER containing lipid mixtures including CHOL.[34,35] These studies reveal that CHOL controls the miscibility of the CER containing lipid mixtures. In previous studies, the phase behavior of lipid mixtures prepared from isolated human CERs or pig CERs in the presence of varying levels of CHOL has been investigated.[32,36] These papers report that (i) in the absence of CHOL, the typical lamellar phases in SC do not form and (ii) addition of a small amount of CHOL (0.2 molar ratio for human CERs (CER/CHOL/FFA (1 : 0.2 : 1)) and 0.4 molar ratio for pig CERs (CER/CHOL/FFA (1 : 0.4 : 1))) triggers the formation of the two lamellar phases. In these studies the effect of CHOL on the formation of the orthorhombic phases has not been examined systematically.[32,36]

The aim of our present study was to examine in more detail the role of CHOL in forming the characteristic SC lipid organization. In contrast to previous studies, we used lipid mixtures prepared with synthetic CERs that allowed forming exclusively either the LPP or the SPP. This offered the possibility to examine the role of CHOL in the formation of the orthorhombic lateral packing in each of these lamellar phases separately. Furthermore, the role of CHOL in the formation of each of these lamellar phases was also examined. Our studies reveal that in the absence of CHOL, the orthorhombic lateral packing as well as the LPP and SPP are not formed. A gradual increase in the level of CHOL enhances the formation of the orthorhombic lateral packing and both lamellar phases (LPP and SPP). These studies therefore suggest that CHOL is a key building block for a proper dense lipid organization in both lamellar phases and that in the absence of CHOL, the CERs and FFAs cannot exert their role in forming a proper skin barrier.

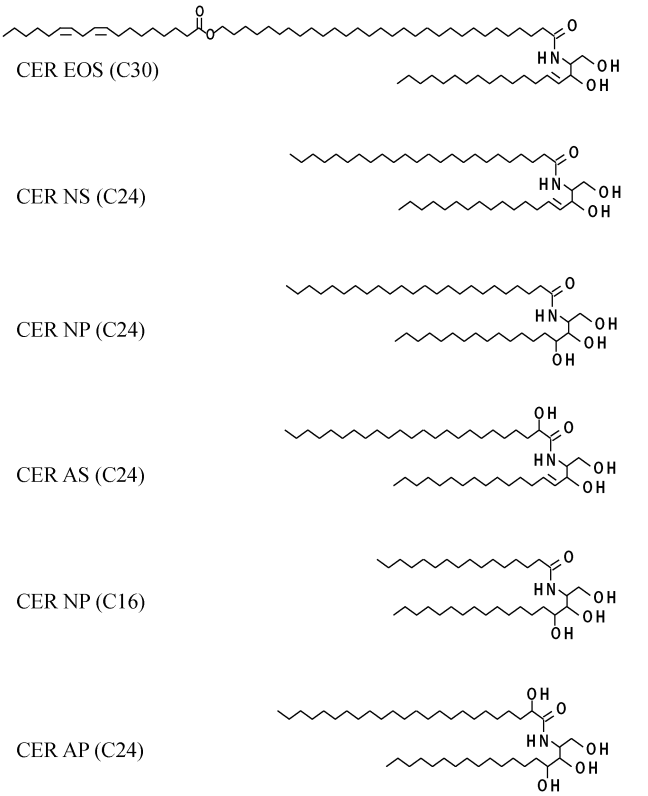

Fig. 1 Molecular structure of the synthetic CERs with their abbreviation of names and chain lengths given within parentheses used in the present study.

2. Experimental

2.1 Materials

The following synthetic CERs were used in our studies: (1) the ester linked omega-hydroxy acyl chain (abbreviation EO, the number between the brackets indicates the number of carbon atoms in the acyl chain (C30)) with a sphingosine chain (abbreviation S, C18) referred to as CER EOS (C30), (2) a non-hydroxy acyl chain (abbreviation N, C24) linked to a sphingosine base (C18) referred to as CER NS (C24), (3) a non-hydroxy acyl chain (C24 or C16) linked to a phytosphingosine base (abbreviation P) referred to as CER NP (C24) and CER NP (C16), respectively, (4) an alpha-hydroxy chain (abbreviation A) linked to a sphingosine base referred to as CER AS (C24) and (5) an alpha-hydroxy acyl chain (C24) linked to a phytosphingosine base referred to as CER AP (C24). The molecular structure of these synthetic CERs are provided in Fig. 1. The CERs were kindly provided by Evonik (Essen, Germany). The various FFAs (palmitic acid (C16 : 0), stearic acid (C18 : 0), arachidic acid (C20 : 0), behenic acid (C22 : 0), tricosanoic acid (C23 : 0), lignoceric acid (C24 : 0), cerotic acid (C26 : 0)) and CHOL are obtained from Sigma-Aldrich Chemie GmbH (Schnelldorf, Germany). Nucleopore polycarbonate filter disks with a pore size of 50 nm were obtained from Whatman (Kent, UK). All solvents were of analytical grade and supplied by Labscan (Dublin, Ireland). The water used was of Millipore quality produced by Milli-Q water filtration system with a resistivity of 18 MΩ cm at 25 °C.

2.2 Preparation of the model lipid mixtures

In order to prepare the model lipid membranes, synthetic CERs, CHOL and FFAs were used. The CERs and FFAs were used in an equimolar ratio while the CHOL level varied systematically. The compositions are provided in Tables 2 and 3. Two different CER compositions were used to prepare the model lipid mixtures. They are referred to as $sCER^{EOS}$ (in the presence of CER EOS) and sCER (in the absence of CER EOS) respectively. The composition of the CER was chosen based on earlier studies, in which we showed that using this composition with 15 mol% CER EOS, the same lamellar phases and lateral packing are formed as observed in human and pig SC, but also in lipid mixtures prepared with isolated pig or human CERs.[32,36,37] To prepare the mixtures only forming the LPP with an equimolar ratio of CER/CHOL/FFA, the CER EOS level was increased to 40% in the CER mixture, while the mixtures only forming the SPP were prepared without the

Table 1 The CER (chain length of the acyl chain is given within parenthesis) and FFA composition and mol% used to prepare the lipid mixtures are provided. The difference between the mixtures is the presence and absence of CER EOS. In the absence of CER EOS, the ratio between the remaining CER subclasses is the same as in the presence of CER EOS

CER name and chain length	mol%	mol%	FFA name and chain length	mol%
CER EOS (C30)	40		Palmitic acid (C16)	1.8
CER NS (C24)	36	60	Stearic acid (C18)	4
CER NP (C24)	11	18	Arachidic acid (C20)	7.7
CER AS (C24)	3	5	Behenic acid (C22)	42.6
CER NP (C16)	6	10	Tricosylic acid (C23)	5.2
CER AP (C24)	4	7	Lignoceric acid (C24)	34.7
			Cerotic acid (C26)	4.1
Total	**100** $\mathbf{sCER^{EOS}}$	**100** **sCER**		**100** **FFA**

presence of CER EOS. The detailed composition in mol% of these two CER mixtures are given in Table 1. The composition of the FFA mixture with their mol% is also provided in Table 1. This FFA composition is based on those reported to be present in the SC.[38] In order to examine the mixing properties of the lipid mixtures, in a few FTIR (Fourier transform infrared) studies, the protonated FFAs were replaced by their deuterated counterparts using the following composition: C16 : 0, C18 : 0, C20 : 0, C22 : 0 and C24 : 0 at molar ratios of 1.8, 4.0, 7.6, 47.8 and 38.8 respectively. In preparing the model lipid mixtures for SAXD (small angle X-ray diffraction) studies, an appropriate amount of individual lipids dissolved in chloroform : methanol (2 : 1) was evaporated under a flow of nitrogen. Then the lipids were redissolved in a hexane : ethanol (2 : 1) solution to a final concentration of 4.5 mg mL^{-1}. This mixture was used to prepare the lipid membranes as described below.

2.3 FTIR sample preparation

In preparing the FTIR samples 1.5 mg of lipids at a concentration of 7.5 mg mL^{-1} were dissolved in chloroform : methanol (2 : 1). This solution was sprayed on an area of 1 × 1 cm^2 on a ZnSe window using a Camag Linomat IV sample applicator (Muttenz, Switzerland). The samples were equilibrated for about 10 minutes between 80–120 °C depending on the composition of the lipid mixtures and cooled gradually to room temperature. Subsequently, the lipid layers were covered with 25 μL deuterated acetate buffer (pH 5.0) and equilibrated at 37 °C for 15 h to fully hydrate the samples. Finally, the samples were cooled to 0 °C prior to the measurements.

2.4 FTIR measurements and data analysis

The FTIR setup consisted of a BIORAD FTS4000 FTIR spectrometer (Cambridge MA, USA) equipped with a broad-band mercury cadmium telluride detector, cooled by liquid nitrogen. The sample cell was closed by two ZnSe windows. The sample was under continuous dry air purge starting 30 minutes before the data acquisition. The spectra were collected in a transmission mode with a co-addition of 256 scans at 1 cm^{-1} resolution during 4 minutes. In order to detect phase transitions, the sample temperature was increased at a heating rate of 0.25 °C min^{-1} resulting in a 1 °C temperature rise per recorded spectrum. The spectra were collected between 0 °C and 90 °C and deconvoluted using a half-width of 4 cm^{-1} and an enhancement factor of 1.7. The software Win-IR pro 3.0 from Biorad was used for FTIR data reduction. The fitting of the FTIR scissoring spectra were performed using the software OriginPro 8.5 from the OriginLab Corporation (Northampton, USA).

2.5 FTIR spectral fitting

The scissoring contours in the FTIR spectra at 25 °C of the various lipid mixtures as reported in Tables 2 and 3 were fitted using the following Lorentzian function:

$$y = y_0 + \left(\frac{2A}{\pi}\right) \cdot \left\{\frac{w}{4(x - x_0)^2 + w^2}\right\}$$

Here y_0 is the offset for baseline correction, A represents the peak area, x_0 is the center of the peak and w is the full width at its half maximum. The fitting procedure (using the software OriginPro 8.5 from the OriginLab Corporation, Northampton, USA) minimizes the deviations between the theoretical and experimental spectra by using the minimization algorithm based on the non-linear least square method. The coefficient of determination (COD) and the χ^2 values were evaluated in order to determine the best-fit results of the original spectra. A value of COD close to 1 indicates a good fit of the data points to the original spectra.

Table 2 The compositions of various $sCER^{EOS}$ containing model lipid mixtures. The lamellar organization with its repeat distances, the unknown phases with their spacings and the lipid lateral packing are provided. The OR/HEX peak ratio as determined by the Lorentzian peak fitting procedure of the FTIR scissoring band spectra at 25 °C are also presented

Composition and molar ratio ($sCER^{EOS}$/CHOL/FFA)	Lamellar phase and/or unknown phases[a] (25 °C)	Repeat distance and/or spacings[a] (nm)	Phase separated CHOL (25 °C)	OR/HEX peak ratio[b] (25 °C)
1 : 0 : 0	Unknown phases[a]	*6.9*,[a] *3.6*[a]	—	0.09
1 : 0 : 1	Unknown phases[a]	*6.5*,[a] *3.9*[a]	—	0.12
1 : 0.05 : 1	LPP, lamellar and unknown phases[a]	13.0, 9.7, *3.9*[a]	—	0.28
1 : 0.1 : 1	LPP	12.7	—	0.29
1 : 0.2 : 1	LPP	12.2	—	0.52
1 : 0.5 : 1	LPP	12.2	+	0.74
1 : 1 : 1	LPP	12.2	+	0.78

[a] The diffraction peaks that cannot be combined with higher diffraction orders attributed to the same phase cannot be assigned to a particular phase and are therefore referred to as unknown phases. The spacings of these unknown phases are provided in italics. [b] The abbreviations OR and HEX stand for orthorhombic and hexagonal lateral packing respectively.

Table 3 The composition and molar ratios used to prepare various sCER containing model membranes (in the absence of CER EOS). The lamellar and unknown phases with their repeat distances and spacings are presented in the table. The OR/HEX peak ratio determined from the spectra collected at 25 °C for the sCER containing lipid mixtures are presented. Several of the phases have repeat distances that do not correspond to the typical SPP repeat distance of approximately 5.3 nm in the synthetic mixtures and therefore these phases are denoted as lamellar phases

Composition and molar ratio (sCER/CHOL/FFA)	Lamellar phases and/or unknown phases[a] (25 °C)	Repeat distances and/or spacings[a] (nm)	Phase separated CHOL (25 °C)	OR/HEX peak ratio (25 °C)
1 : 0 : 0	Lamellar and unknown phases[a]	*5.4*,[a] 4.4	—	0.06
1 : 0 : 1	Lamellar and unknown phases[a]	5.7, *4.4*[a]	—	0.07
1 : 0.05 : 1	Lamellar and unknown phases[a]	*5.8*,[a] 4.4, 3.9	—	0.37
1 : 0.1 : 1	Lamellar and unknown phases[a]	5.7, *4.4*[a]	—	0.39
1 : 0.2 : 1	SPP	5.3	—	0.27
1 : 0.5 : 1	SPP	5.3	—	0.34
1 : 1 : 1	SPP	5.3	+	0.41

[a] No higher order reflections are observed, therefore these numbers refer to the spacing corresponding to the single diffraction peak of the particular phase, referred to as the unknown phase.

This fitting procedure allows multiple peak fittings for a certain region of the spectra, *e.g.* 1460 to 1480 cm^{-1} of the scissoring band. The CH_2 scissoring vibration allows us to monitor the orthorhombic and hexagonal lateral packing separately as the contour from the hexagonal lateral packing occurs at ~1467 cm^{-1}, which is at a different position than the orthorhombic doublet with peak positions at around 1463 and 1473 cm^{-1}. The area of each individual peak that contributed to the total peak area was calculated after the fitting procedure. For calculating the orthorhombic peak area, the total area of components 1 and 3 was determined, while the area of component 2 represents the peak area attributed to a hexagonal packing (Fig. 3). To examine the effect of CHOL on the formation of the orthorhombic phase in the lipid mixtures, the ratio between the peak areas of orthorhombic and hexagonal contours was calculated.

2.6 Preparation of the model membranes for SAXD studies

To prepare the lipid membranes for SAXD studies, the lipid mixtures were sprayed on top of Whatman nucleopore polycarbonate filter disks using a Camag Linomat IV (Muttenz, Switzerland) sample applicator with an extended *y*-axis arm.[39] A Hamilton syringe (100 μL) was inserted into the Linomat and used to spray a selected volume of sample solution from a distance of approximately 1 mm onto the porous filter substrate under a stream of nitrogen flow. With the *y*-axis arm, the Linomat is capable of spraying lipids in a square shape (8 by 8 mm), by a continuous zigzag movement. The temperature during the spraying was 25 °C and the spraying flow rate was set to 5.0 μL min^{-1}. The total amount of lipids sprayed per membrane was about 0.9 mg. After spraying, the membrane was equilibrated for about 12 minutes between 75–120 °C. The equilibration temperature depended on the selected lipid mixtures, but was close to the temperature at which melting occurs. After equilibration, the membranes were gradually cooled to room temperature before the measurements.

2.7 SAXD studies

SAXD was used to examine the long range ordering. The scattering intensity I (in arbitrary units) was measured as a function of the scattering angle (θ), from which the scattering vector (q) was calculated (in reciprocal nm). The latter is defined as $q = (4\pi \sin\theta)/\lambda$, in which λ is the wavelength. From the positions of a series of equidistant peaks (q_n), the periodicity (d) of a lamellar phase was calculated using the equation $d = 2n\pi/q_n$, with n being the order number of the diffraction peak. When a particular peak position (reciprocal space) is related to the real space, we use the term spacing, which is equal to $2\pi/q$ at that peak position. One-dimensional intensity profiles were obtained by transformation of the 2D SAXD detector pattern from Cartesian (x,y) to polar (ρ,θ) coordinates and subsequently integrating over θ. All measurements were performed at the European Synchrotron Radiation Facility (ESRF) located in Grenoble, France using station BM26B. The wavelength of the X-ray and the sample-to-detector distance were 0.1033 nm and 2.1 m, respectively. The diffraction data were collected on a PILATUS 1M detector (1043 × 981 pixels) and 172 μm spatial resolution. The calibration of this detector was performed using silver behenate and aluminum oxide. The lipid membrane was mounted parallel to the primary beam in a sample holder with mica windows. All the diffraction data were collected for about 5 minutes at 25 °C.

3. Results

3.1 Lateral packing of the various lipid compositions

The FTIR scissoring vibrations provide information about the lateral packing present in the lipid lamellae. When the lipid tails are hexagonally packed, a singlet is observed at around ~1467 cm^{-1} while lipid tails partly adopting an orthorhombic packing show a broadening or splitting of the contours due to the interaction of the adjacent chains *via* the short range coupling. An orthorhombic packing results in two peaks at approximately 1463 and 1473 cm^{-1}.[40] The CH_2 scissoring frequencies in the spectra of all the $sCER^{EOS}$ containing lipid mixtures are shown in Fig. 2. As all relevant changes in the scissoring frequencies are observed below 60 °C, only the curves below this temperature are presented.

First the spectra without CHOL are presented. In the spectra of the $sCER^{EOS}$, an asymmetric scissoring vibration peak with a maximum at ~1467 cm^{-1} is observed in the temperature range between 20 and 60 °C, demonstrating the presence of mainly a hexagonal lateral packing (Fig. 2A). The asymmetry is due to a

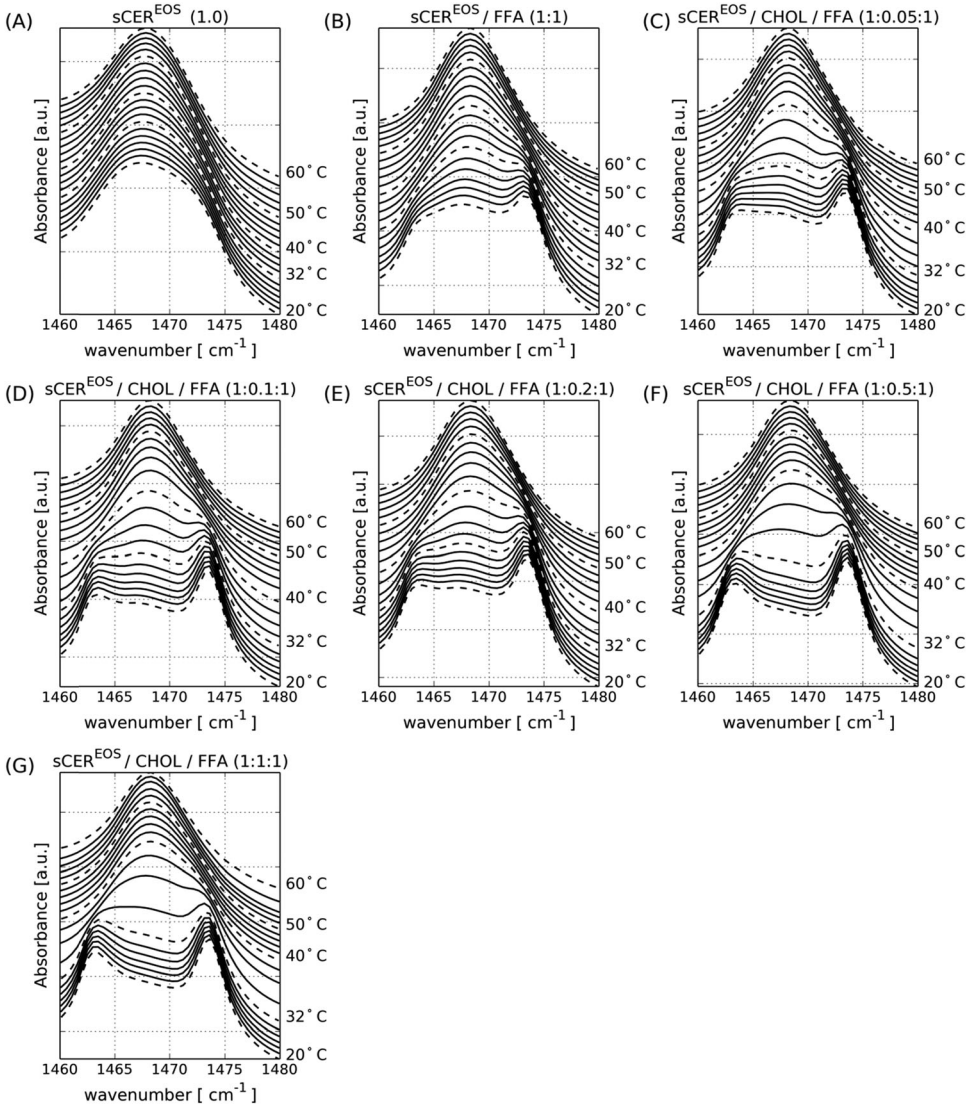

Fig. 2 The thermotropic CH_2 scissoring vibration frequencies of the CER EOS containing lipid mixtures ($sCER^{EOS}$) as a function of temperature. The spectra are shown from the 20 to 60 °C temperature region. The 32 °C is also shown as a dashed line as this represents the average skin temperature.

small shoulder at ~1473 cm^{-1}. The spectrum of the scissoring vibration of the equimolar $sCER^{EOS}$/FFA exhibits the presence of a weak doublet at around 1463 and 1473 cm^{-1} at 20 °C (Fig. 2B), the latter peak of which is stronger. This indicates that a small fraction of lipids adopts an orthorhombic lateral packing at this temperature. In between the doublet a high strong singlet is observed at around 1467 cm^{-1} demonstrating that a large fraction of lipids forms a hexagonal lateral packing. The 1463 cm^{-1} band disappears at around 32 °C and the band at ~1473 is present until 40 °C. At a temperature above 40 °C, only a singlet is observed at a frequency of ~1467 cm^{-1}, suggesting that the lipids are participating in the hexagonal phase only.

The spectrum of the 0.05 molar ratio CHOL ($sCER^{EOS}$/CHOL/FFA (1 : 0.05 : 1)) at 20 °C resembles the spectrum of the equimolar $sCER^{EOS}$/FFA, although the peak intensities of the doublet at ~1463 and 1473 cm^{-1} slightly enhance, indicating that an increased fraction of lipids adopts the orthorhombic packing compared to the equimolar $sCER^{EOS}$/FFA (Fig. 2C). The doublet remains visible until 38 °C. The 1463 cm^{-1} and 1473 cm^{-1} bands disappear at 38 °C and 42 °C, respectively. Beyond this temperature only a singlet is present at ~1467 cm^{-1}. A small increment of the CHOL level to the compositions of $sCER^{EOS}$/CHOL/FFA (1 : 0.1 : 1) and $sCER^{EOS}$/CHOL/FFA (1 : 0.2 : 1) increases the intensity of the 1463 and 1473 cm^{-1} bands further. At 40 °C, the 1463 cm^{-1} band disappears for both lipid mixtures and at 42 °C, the 1473 cm^{-1} band vanishes as well and only a singlet at ~1467 cm^{-1} remains until 60 °C (Fig. 2D and E). A further increment of CHOL levels resulting in the compositions $sCER^{EOS}$/CHOL/FFA (1 : 0.5 : 1) and $sCER^{EOS}$/CHOL/FFA (1 : 1 : 1) exhibit a stronger doublet at positions 1463 and 1473 cm^{-1} at 20 °C, indicative of a further increased level of lipids adopting an orthorhombic packing (Fig. 2F and G). The 1463 cm^{-1} and 1473 cm^{-1} contours disappear at 38 °C and 40 °C after which only a singlet is observed.

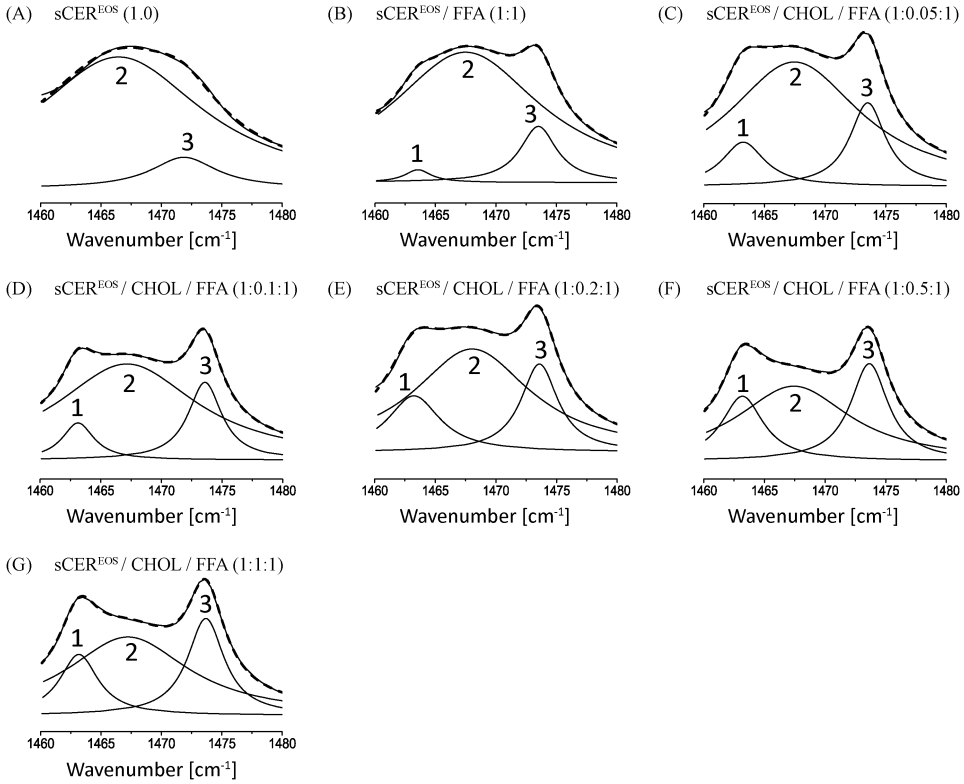

Fig. 3 The FTIR CH_2 scissoring vibration spectra in the region of 1460 to 1480 cm^{-1} at 25 °C (solid lines) for various $sCER^{EOS}$ containing lipid mixtures. The dashed lines indicate the best-fit as determined by the Lorentzian function. The individual components that make up the overall Lorentzian best-fit are designated by 1, 2 and 3. Components 1 and 3 with their approximate scissoring band frequencies of around 1463 and 1473 cm^{-1} are assigned to the orthorhombic phase while component 3 with its approximate position at 1467 cm^{-1} to the hexagonal phase.

The scissoring spectra of the sCER containing lipid mixtures have also been measured and are presented in the Fig. S1 (ESI†). The spectra of these lipid mixtures show a similar trend concerning the scissoring vibrations as those in the spectra of mixtures in the presence of CER EOS ($sCER^{EOS}$): an increase in the CHOL levels results in a higher level of lipids assembling in an orthorhombic lateral packing. However, the level of lipids adopting an orthorhombic phase is lower than in $sCER^{EOS}$ containing mixtures.

In order to examine the contribution of the orthorhombic and hexagonal lateral packing in the lipid mixtures quantitatively, the FTIR scissoring spectra at 25 °C were fitted with a Lorentzian function. Fig. 3 displays the original and the fitted spectra with their individual components of the $sCER^{EOS}$ containing lipid mixtures. The fitting of the original spectra results in COD values very close to 1 (in all cases, 0.999 with variations in the 4th and 5th decimal places), which indicates that the peak fittings are excellent.

Fig. 3A shows that the scissoring band in the spectrum of $sCER^{EOS}$ is formed by the coexistence of two components. Component 2 has a much higher peak area compared to component 3, indicative of a high fraction of lipids adopting a hexagonal phase. Fig. 3B represents scissoring band formation in the spectrum of the equimolar $sCER^{EOS}$/FFA mixture. Compared to the $sCER^{EOS}$ the contribution of component 2 is slightly reduced, the contribution of component 1 is introduced and that of component 3 is increased. An increase in the CHOL level enhances the contribution of components 1 and 3 while reducing component 2 (Fig. 3C–G), suggesting a gradual increase of orthorhombic packing at the expense of the hexagonal as evident from the OR/HEX peak ratio given in Table 2. The ratios between OR/HEX contour areas are presented in Table 2 and shown in a quantitative manner that an increase in CHOL results in an increased population of lipids adopting the orthorhombic phase.

The Lorentzian fitting of the scissoring spectra collected at 25 °C for the various lipid mixtures in the absence of CER EOS (sCER) is presented in the Fig. S2 (ESI†). The OR/HEX peak ratio for these lipid mixtures are provided in Table 3. CHOL contributes to the orthorhombic domain formation in the sCER containing lipid mixtures, especially when adding small levels of CHOL (evident from the OR/HEX peak ratio in Table 3).

3.2 CHOL is necessary for the formation of the LPP

SAXD provides information about the long range ordering in the lipid mixtures and the presence of the lamellar phases. The detected lipid lamellar phases with their corresponding repeat distances of the various lipid membranes in the presence of CER EOS are reported in Table 2. The corresponding diffraction patterns of these lipid membranes are presented in Fig. 4.

In the diffraction pattern of the $sCER^{EOS}$ mixture (Fig. 4A), the width at half maximum of the peaks is broad and the peaks

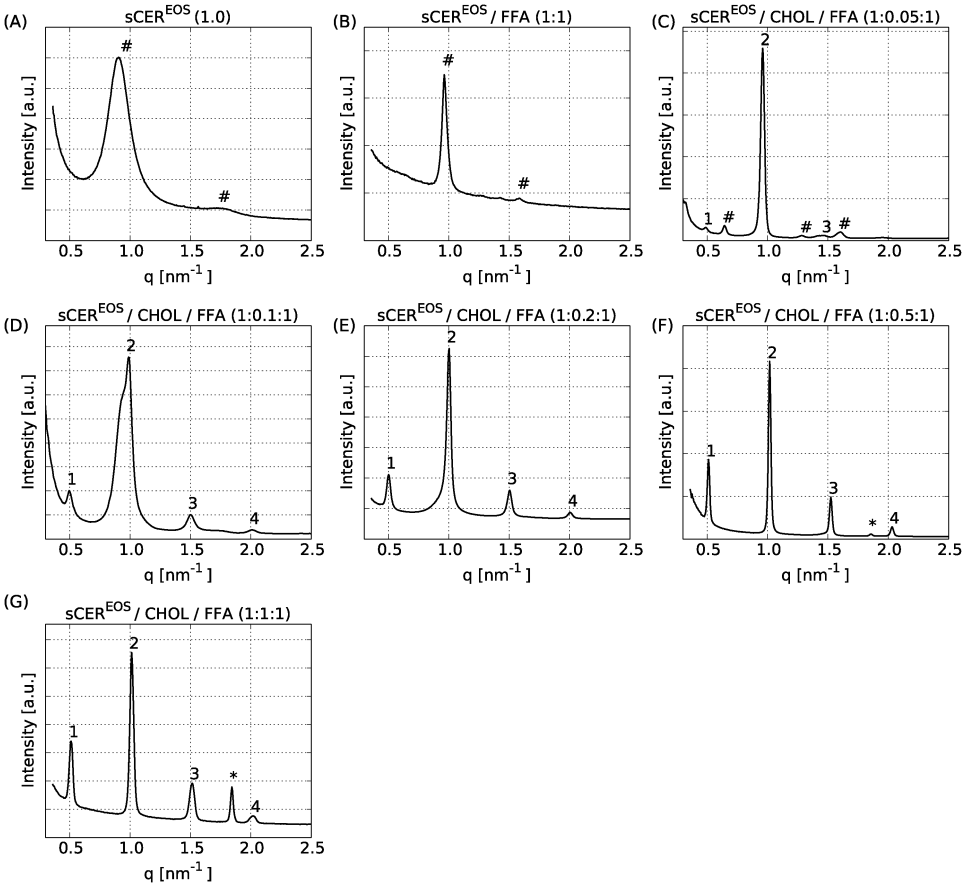

Fig. 4 SAXD diffraction profile of various $sCER^{EOS}$ containing lipid membranes used in our study. The figure title describes the different lipid membranes prepared. In the SAXD profiles, the arabic numbers (1, 2, 3...) indicate the different diffraction orders of the LPP. The peaks originating from the crystalline CHOL domains are indicated by the asterisk (*). The peaks attributed to other phases than LPP or CHOL are indicated by the hash sign (#).

are positioned at q = 0.90 and 1.72 nm^{-1}. The positions of these two peaks correspond to spacings at 6.9 and 3.6 nm, respectively. These peaks probably do not belong to one phase. As no higher order reflections are present in the diffraction pattern, a more detailed interpretation is not possible. After the addition of FFA resulting in an equimolar $sCER^{EOS}$/FFA mixture two peaks are visible at the diffraction pattern at q = 0.96 and 1.59 nm^{-1} (Fig. 4B) corresponding to spacings of 6.5 nm and 3.9 nm. Again, these peaks cannot be attributed to a particular phase as no higher order diffraction patterns are present.

To determine the minimum level of CHOL required for the formation of LPP, the X-ray diffraction patterns of the $sCER^{EOS}$/CHOL/FFA mixtures with an increasing CHOL level was also measured. The lipid mixture at a molar ratio $sCER^{EOS}$/CHOL/FFA (1 : 0.05 : 1) exhibits a drastic change in phase behavior. The diffraction pattern is characterized by the presence of three diffraction orders at q = 0.48, 0.96 and 1.45 nm^{-1} with a repeat distance of 13.0 nm, demonstrating the formation of the LPP (Fig. 4C). However, besides the presence of the LPP, two additional phases are also observed as indicated by diffraction peaks at q = 0.64 and 1.28 nm^{-1} for the 1st and 2nd order of this phase with a repeat distance of 9.7 nm and at q = 1.60 nm^{-1}, an unknown phase corresponding to a 3.9 nm spacing. A further increase in the CHOL level resulting in a mixture of $sCER^{EOS}$/CHOL/FFA (1 : 0.1 : 1) shows the presence of four diffraction orders at q values of 0.49, 0.98, 1.49 and 1.99 nm^{-1} that can be attributed to a lamellar phase with a repeat distance of 12.7 nm, indicative of the presence of the LPP (Fig. 4D). Furthermore, a shoulder is observed on the left side of the 2nd order peak (at 0.98 nm^{-1}) suggesting the formation of another phase. Upon further increasing the CHOL content, the X-ray diffraction profiles demonstrate the formation of the LPP in the mixtures $sCER^{EOS}$/CHOL/FFA with molar ratios of 1 : 0.2 : 1, 1 : 0.5 : 1 and 1 : 1 : 1. In these mixtures the repeat distance of the LPP is 12.2 nm. This is based on diffraction peaks at q positions of 0.51, 1.01, 1.51 and 2.02 nm^{-1} for the 1st, 2nd, 3rd and 4th order diffraction peaks respectively (Fig. 4E, F and G). At a 0.5 molar ratio of CHOL in the lipid mixture ($sCER^{EOS}$/CHOL/FFA (1 : 0.5 : 1)), the crystalline CHOL phase is separated (Fig. 4F). In the diffraction pattern of the equimolar ratio of $sCER^{EOS}$/CHOL/FFA, the peaks attributed to phase-separated crystalline CHOL domains are also clearly visible in the SAXD pattern (Fig. 4G).

The repeat distances of the lamellar phases detected for various sCER containing lipid mixtures are presented in Table 3. The corresponding diffraction patterns are presented in the Fig. S3 (ESI†). Similar to $sCER^{EOS}$/CHOL/FFA lipid mixtures, at the levels of CHOL lower than sCER/CHOL/FFA (1 : 0.2 : 1), the diffraction patterns show diffraction peaks indicating the presence of several phases without the presence of phase separated CHOL and SPP.

When the CHOL level reaches a ratio of sCER/CHOL/FFA (1 : 0.2 : 1), the lipids assemble in the SPP. At CHOL levels higher than sCER/CHOL/FFA (1 : 0.5 : 1), the phase separation of CHOL occurs.

4. Discussion

In our current study using model lipid mixtures and by adjusting the CER composition, we were able to form either the LPP or the SPP, both present in the lipid matrix in SC.[9] In order to be able to form only the SPP, lipid mixtures in the absence of CER EOS were examined. As far as the LPP is concerned, it has been reported that an increment in the level of CER EOS in the lipid mixtures enhances the formation of the LPP at the expense of the SPP.[41] We selected a 40 mol% CER EOS level as lipids adopt only the LPP. This composition has also been used in another study from our group to examine the localization of the lipids in the unit cell of the LPP (EH Mojumdar, GS Gooris, JA Bouwstra, unpublished work). As currently there is very little known about the impact of increasing levels of CHOL on the lipid organization, our aim was to investigate the role of CHOL in the formation in each of the lamellar phases and their corresponding lateral packing. This will provide more insight into the interaction of CHOL with CERs and/or FFAs. The interaction of CHOL with the phospholipids has been studied well. CHOL is involved in the formation of the lipid rafts by ordering the liquid phase. However, it has also been reported that the supplementation of CHOL to phospholipids forming a hexagonal (gel) phase induces the formation of a liquid ordered phase.[42–47] The results presented in this paper are in contrast with the latter observations as discussed below.

4.1 CHOL ensures a proper lipid organization in the LPP

CHOL induces an orthorhombic lateral packing in the LPP. The fraction of lipids adopting an orthorhombic lateral packing is gradually augmented when the level of CHOL is progressively increased in the $sCER^{EOS}$ containing lipid mixtures. The presence of a solid phase has also been examined when using solid-state NMR studies: CHOL in the presence of CERs and FFAs exhibits a 'solid phase' in which the lipid motions are inhibited.[48,49] Our results also demonstrate that besides an increase in lipid density, CHOL is also crucial for the formation of the LPP: a minimum CHOL level of $sCER^{EOS}$/CHOL/FFA (1 : 0.2 : 1) is obligatory for the formation of this phase. In addition, we also investigated whether the CER head-group variation is important for the formation of the LPP. Therefore, we have examined whether lipid mixtures containing only CER NS and CER EOS form the LPP. Both of these CER subclasses do have the same head-group architecture: an acyl chain linked to a sphingosine base. Our studies showed that lipid mixtures prepared from CERs (CER EOS and CER NS in a 0.4/0.6 molar ratio), CHOL and FFAs in an equimolar ratio form the LPP (EH Mojumdar, GS Gooris, JA Bouwstra, unpublished work). This suggests that variation in the CER head-group architecture is not a prerequisite for the formation of the LPP. However, also by using these two CER subclasses in the absence of CHOL, no LPP can be formed. This shows again that the presence of CHOL is crucial to the formation of the LPP.

4.2 The effect of CHOL on the formation of the crystalline SPP

When considering the effect of CHOL, the lipid mixtures forming only the SPP show a similar trend as observed in the lipid mixtures forming the LPP. CHOL is required for the formation of the orthorhombic lateral packing in the SPP. In previous neutron diffraction studies and model calculations it was shown that CHOL fits excellently in the unit cell of the SPP. Neutron diffraction studies revealed the location of CHOL, lignoceric acid (FFA C24 : 0) and CER NS in this unit cell and suggest that a single CHOL molecule is opposing two long chain fatty acids in the unit cell of the SPP.[30] In fact the short length of CHOL ($\sim$17 Å) compensates for the long fatty acids extending the center of the unit cell. Therefore the localization of CHOL in the gaps opposite to the very long chain FFAs may perhaps contribute to the denser packing of the acyl chains enabling the chains to form an orthorhombic lateral packing in the SPP. This also implies that in the sCER/CHOL/FFA mixture, the maximum level of CHOL is approximately 50% of that of the level of FFA. This is in agreement with our findings that the maximum level of CHOL in the sCER/CHOL/FFA mixture is 1 : 0.5 : 1.

The interaction of CHOL with the phospholipids has been studied extensively. It has been reported that the supplementation of CHOL to phospholipids in a hexagonal (gel) packing destabilizes the hexagonal packing and induces the formation of a liquid ordered phase.[42–45,47,50,51] When the phospholipids are in a liquid phase, CHOL enhances the ordering of the lipid tails by the formation of the liquid ordered phase.[52–55] As CER:FFA mixtures form a crystalline phase, our findings are in contrast to those observed in phospholipid systems as a gradual increment of CHOL to the lipid mixtures enhances the fraction of lipids forming a highly dense orthorhombic packing and does not result in a liquid ordered phase. An unusual role of CHOL was also observed when mixtures were prepared from pseudo-ceramide, stearic acid and CHOL: it was reported that CHOL increases the mobility of the hydrocarbon chain in the lipid mixture.[56] This demonstrates that the phase behavior of mixtures with pseudo-ceramide, CHOL and FFA is different from that of mixtures prepared from CERs, CHOL and FFA. This may also indicate that pseudo-ceramides when used in formulations for topical application may have an entire different effect when intercalated in the lipid bilayers in the SC. The difference is most likely caused by a difference in the molecular architecture of the pseudo-CER. A difference in the preparation method is not very likely as all the studies focusing on the molecular organization in mixtures with CERs report ordered crystalline phases.[33,57–60] These studies therefore demonstrate that CHOL plays an important role in the CER containing lipid mixtures and in the formation of the proper lipid organization.

4.3 Similarities and differences in the lipid organization between the LPP and SPP

Although the effect of CHOL on the formation of the LPP and SPP and their corresponding lateral organization is very similar, there are also differences observed between the LPP and SPP: (i) a substantial higher fraction of lipids adopt an orthorhombic lateral packing in the LPP compared to that in the SPP. The presence of

long acyl chains of CER EOS may contribute to the increased level of lipids forming an orthorhombic packing in the LPP: an increased hydrocarbon chain length of the CER EOS increases the van der Waals interactions and this reduces the inter-chain distance as has been reported previously.[61] This also indicates that the chain length distribution plays an important role in the formation of the orthorhombic lateral packing.[62] (ii) Due to the ~13 nm repeat distance, the arrangement of lipids is expected to be very different in the LPP and SPP. Previous studies indicated that the unit cell of the LPP consists of three lipid layers.[63] Neutron diffraction studies performed with either deuterated CER NS or perdeuterated FFA C24 : 0 in the lipid mixture suggests that the majority of CER NS and FFA C24 are located in the central layer of the unit cell of the LPP and substantially interdigitate (E. H. Mojumdar, G. S. Gooris, D. J. Barlow, M. J. Lawrence, B. Deme, J. A. Bouwstra, *Biophys. J.*, in press). This makes the localization of CHOL in this central layer highly unlikely. Therefore, unlike the lipid arrangement in the unit cell of the SPP, in which the CHOL head group is at a small distance from the unit cell boundary intercalated between the FFA and CERs,[30] the CHOL in the LPP is expected to be situated in the two outer layers of the LPP where it probably opposes the chains of CER and/or FFA directing from the unit cell border of the LPP.

4.4 CHOL does not induce phase separation

In order to examine the mixing properties of the lipid mixtures in the presence of CHOL, using the equimolar sCER^{EOS}/CHOL/FFA and sCER/CHOL/FFA, the protonated FFAs were replaced with their deuterated counterparts and FTIR studies were performed (Fig. 5). When replacing protonated FFAs by their deuterated counterparts in the lipid mixtures, neighboring protonated CER chains and deuterated FFA chains do not result in the short range coupling of the vibrations and consequently when participating in one lattice a singlet of scissoring vibrations in the spectrum is expected. However if CERs and FFAs form separate phases, a doublet is expected in the scissoring band region (1080–1100 cm^{-1} wavenumber).[64] In the equimolar sCER^{EOS}/CHOL/FFA a weak splitting is observed in this region (Fig. 5A), while a single peak is observed in the equimolar sCER/CHOL/FFA mixture (Fig. 5B). This indicates that the CERs and FFAs in the presence of CHOL participate in the same orthorhombic lattice. When examining the weak doublet in the FTIR spectrum of sCER^{EOS}/CHOL/FFA (1 : 1 : 1) as a function of temperature, the weak splitting of the CD_2 scissoring band disappears upon increasing the temperature to around 30 °C. This low temperature suggests that a very small fraction of FFA chains are packed close to each other, but do not form a separate orthorhombic packing. It has been reported that CHOL enhances the mixing properties of the lipids and plays a significant role in controlling the miscibility of the lipids also in less complex mixtures.[35] These results therefore may suggest that irrespective of complex or single CER containing lipid mixtures, CHOL induces the participation of other lipids in a single lattice by avoiding phase separation in the lipid mixtures.

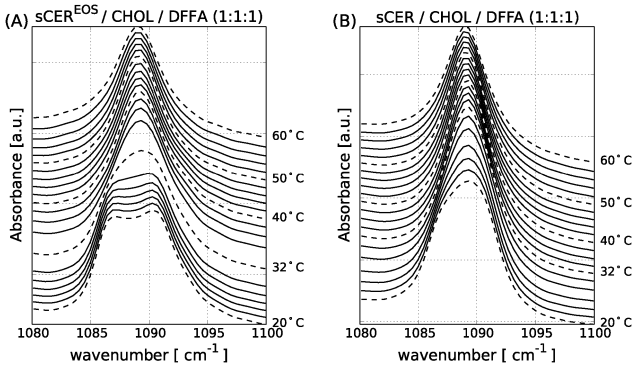

Fig. 5 The FTIR scissoring spectra of the lipid mixtures with deuterated FFA from 20 to 60 °C. The figure describes the lipid composition and molar ratios used to examine the mixing properties of the lipid mixture. At temperatures below 32 °C only a weak splitting is observed in mixtures with sCER^{EOS}, while a slightly broader single peak is observed in mixtures prepared with sCERs. This indicates that FFA and CER participate in one lattice.

4.5 Comparison with results obtained using theoretical simulations

The results we obtained in our present study are in agreement with theoretical simulations reported in the literature.[65] In simulation studies carried out for the CER NS/CHOL/FFA C24 mixtures, it was shown that the presence of CHOL squashes the central region of the bilayer comprising of primarily CER tails. This was shown to enhance the interdigitation and ordering of the tails of the opposing CERs in the central region and reduces the bilayer thickness.[65] In our present study, we also observe that the addition of CHOL reduces the repeat distance of the SPP lipid lamellae. This may be due to the higher density in the lipid tails of CERs and FFAs.

5. Conclusions

In the present study, we examined the contribution of CHOL to the lipid organization of synthetic CER containing lipid mixtures. Our studies revealed that, CHOL is an important building block for the formation of the orthorhombic lateral packing of the lipid tails. Furthermore CHOL also induces the formation of both the SPP and LPP. Therefore, the presence of CHOL is a prerequisite for the characteristic SC lipid organization, stabilizes the structure and thereby contributes to the skin lipid barrier.

Acknowledgements

We like to thank the company Evonik (Essen, Germany) for their generous provision of CERs and the personnel at the DUBBLE beam line 26b at the ESRF located at Grenoble, France for their assistance during the X-ray diffraction measurements.

References

1 P. W. Wertz and B. van den Bergh, *Chem. Phys. Lipids*, 1998, **91**, 85–96.
2 H. E. Boddé, I. van den Brink, H. K. Koerten and F. H. N. de Haan, *J. Controlled Release*, 1991, **15**, 227–236.

3 P. Talreja, G. Kasting, N. Kleene, W. Pickens and T.-F. Wang, *AAPS PharmSciTech*, 2001, **3**, 48–56.
4 P. W. Wertz, M. C. Miethke, S. A. Long, J. S. Strauss and D. T. Downing, *J. Invest. Dermatol.*, 1985, **84**, 410–412.
5 K. J. Robson, M. E. Stewart, S. Michelsen, N. D. Lazo and D. T. Downing, *J. Lipid Res.*, 1994, **35**, 2060–2068.
6 M. E. Stewart and D. T. Downing, *J. Lipid Res.*, 1999, **40**, 1434–1439.
7 Y. Masukawa, H. Narita, E. Shimizu, N. Kondo, Y. Sugai, T. Oba, R. Homma, J. Ishikawa, Y. Takagi, T. Kitahara, Y. Takema and K. Kita, *J. Lipid Res.*, 2008, **49**, 1466–1476.
8 A. Weerheim and M. Ponec, *Arch. Dermatol. Res.*, 2001, **293**, 191–199.
9 J. A. Bouwstra, G. S. Gooris, J. A. van der Spek and W. Bras, *J. Invest. Dermatol.*, 1991, **97**, 1005–1012.
10 J. A. Bouwstra, G. S. Gooris, W. Bras and D. T. Downing, *J. Lipid Res.*, 1995, **36**, 685–695.
11 M. Boncheva, F. Damien and V. Normand, *Biochim. Biophys. Acta, Biomembr.*, 2008, **1778**, 1344–1355.
12 B. Ongpipattanakul, M. L. Francoeur and R. O. Potts, *Biochim. Biophys. Acta, Biomembr.*, 1994, **1190**, 115–122.
13 G. S. K. Pilgram, A. M. E.-v. Pelt, J. A. Bouwstra and H. K. Koerten, *J. Invest. Dermatol.*, 1999, **113**, 403–409.
14 J. A. Bouwstra, G. S. Gooris, M. A. S.-d. Vries, J. A. van der Spek and W. Bras, *Int. J. Pharm.*, 1992, **84**, 205–216.
15 M. Janssens, J. van Smeden, G. S. Gooris, W. Bras, G. Portale, P. J. Caspers, R. J. Vreeken, T. Hankemeier, S. Kezic, R. Wolterbeek, A. P. Lavrijsen and J. A. Bouwstra, *J. Lipid Res.*, 2012, **53**, 2755–2766.
16 D. Groen, D. S. Poole, G. S. Gooris and J. A. Bouwstra, *Biochim. Biophys. Acta, Biomembr.*, 2011, **1808**, 1529–1537.
17 R. O. Potts and M. L. Francoeur, *Proc. Natl. Acad. Sci. U. S. A.*, 1990, **87**, 3871–3873.
18 F. Damien and M. Boncheva, *J. Invest. Dermatol.*, 2010, **130**, 611–614.
19 K. R. Feingold and P. M. Elias, *Biochim. Biophys. Acta, Mol. Cell Biol. Lipids*, 2014, **1841**, 280–294.
20 K. R. Feingold, M. Q. Man, G. K. Menon, S. S. Cho, B. E. Brown and P. M. Elias, *J. Clin. Invest.*, 1990, **86**, 1738–1745.
21 I. Iwai, H. Han, L. d. Hollander, S. Svensson, L.-G. Ofverstedt, J. Anwar, J. Brewer, M. Bloksgaard, A. Laloeuf, D. Nosek, S. Masich, L. A. Bagatolli, U. Skoglund and L. Norlen, *J. Invest. Dermatol.*, 2012, **132**, 2215–2225.
22 N. Kučerka, D. Marquardt, T. A. Harroun, M.-P. Nieh, S. R. Wassall, D. H. de Jong, L. V. Schäfer, S. J. Marrink and J. Katsaras, *Biochemistry*, 2010, **49**, 7485–7493.
23 N. Kučerka, D. Marquardt, T. A. Harroun, M.-P. Nieh, S. R. Wassall and J. Katsaras, *J. Am. Chem. Soc.*, 2009, **131**, 16358–16359.
24 T. A. Harroun, J. Katsaras and S. R. Wassall, *Biochemistry*, 2006, **45**, 1227–1233.
25 J. A. Bouwstra, G. S. Gooris, F. E. R. Dubbelaar, A. M. Weerheim, A. P. IJzerman and M. Ponec, *J. Lipid Res.*, 1998, **39**, 186–196.
26 M. Rabionet, K. Gorgas and R. Sandhoff, *Biochim. Biophys. Acta, Mol. Cell Biol. Lipids*, 2014, **1841**, 422–434.
27 J. van Smeden, L. Hoppel, R. van der Heijden, T. Hankemeier, R. J. Vreeken and J. A. Bouwstra, *J. Lipid Res.*, 2011, **52**, 1211–1221.
28 D. Groen, G. S. Gooris, D. J. Barlow, M. J. Lawrence, J. B. van Mechelen, B. Demé and J. A. Bouwstra, *Biophys. J.*, 2011, **100**, 1481–1489.
29 R. Jennemann, M. Rabionet, K. Gorgas, S. Epstein, A. Dalpke, U. Rothermel, A. Bayerle, F. van der Hoeven, S. Imgrund, J. Kirsch, W. Nickel, K. Willecke, H. Riezman, H.-J. Gröne and R. Sandhoff, *Hum. Mol. Genet.*, 2012, **21**, 586–608.
30 E. H. Mojumdar, D. Groen, G. S. Gooris, D. J. Barlow, M. J. Lawrence, B. Deme and J. A. Bouwstra, *Biophys. J.*, 2013, **105**, 911–918.
31 J. van Smeden, W. A. Boiten, T. Hankemeier, R. Rissmann, J. A. Bouwstra and R. J. Vreeken, *Biochim. Biophys. Acta, Mol. Cell Biol. Lipids*, 2014, **1841**, 70–79.
32 J. A. Bouwstra, G. S. Gooris, F. E. R. Dubbelaar and M. Ponec, *J. Lipid Res.*, 2001, **42**, 1759–1770.
33 X. Chen, S. Kwak, M. Lafleur, M. Bloom, N. Kitson and J. Thewalt, *Langmuir*, 2007, **23**, 5548–5556.
34 J. Zbytovská, M. A. Kiselev, S. S. Funari, V. M. Garamus, S. Wartewig, K. Palát and R. Neubert, *Colloids Surf., A*, 2008, **328**, 90–99.
35 H.-C. Chen, R. Mendelsohn, M. E. Rerek and D. J. Moore, *Biochim. Biophys. Acta, Biomembr.*, 2001, **1512**, 345–356.
36 J. A. Bouwstra, G. S. Gooris, K. Cheng, A. Weerheim, W. Bras and M. Ponec, *J. Lipid Res.*, 1996, **37**, 999–1011.
37 M. W. de Jager, G. S. Gooris, M. Ponec and J. A. Bouwstra, *J. Lipid Res.*, 2005, **46**, 2649–2656.
38 P. W. Wertz and D. T. Downing, *Oxford University Press*, New York, 1991, pp. 205–236.
39 D. Groen, G. S. Gooris, M. Ponec and J. A. Bouwstra, *Biochim. Biophys. Acta, Biomembr.*, 2008, **1778**, 2421–2429.
40 R. Mendelsohn, G. L. Liang, H. L. Strauss and R. G. Snyder, *Biophys. J.*, 1995, **69**, 1987–1998.
41 M. de Jager, G. Gooris, M. Ponec and J. Bouwstra, *J. Invest. Dermatol.*, 2004, **123**, 911–916.
42 R. A. Demel and B. De Kruyff, *Biochim. Biophys. Acta, Rev. Biomembr.*, 1976, **457**, 109–132.
43 T. P. W. McMullen and R. N. McElhaney, *Curr. Opin. Colloid Interface Sci.*, 1996, **1**, 83–90.
44 H. Ohvo-Rekilä, B. Ramstedt, P. Leppimäki and J. Peter Slotte, *Prog. Lipid Res.*, 2002, **41**, 66–97.
45 T. McMullen, R. Lewis and R. McElhaney, *Curr. Opin. Colloid Interface Sci.*, 2004, **8**, 459–468.
46 H. Martinez-Seara, T. Róg, M. Karttunen, I. Vattulainen and R. Reigada, *PLoS One*, 2012.
47 N. Kahya and P. Schwille, *J. Fluoresc.*, 2006, **16**, 671–678.
48 N. Kitson, J. Thewalt, M. Lafleur and M. Bloom, *Biochemistry*, 1994, **33**, 6707–6715.
49 A. C. Rowat, N. Kitson and J. L. Thewalt, *Int. J. Pharm.*, 2006, **307**, 225–231.
50 T. P. W. McMullen, R. N. A. H. Lewis and R. N. McElhaney, *Biochemistry*, 1993, **32**, 516–522.
51 D. A. Mannock, R. N. A. H. Lewis, T. P. W. McMullen and R. N. McElhaney, *Chem. Phys. Lipids*, 2010, **163**, 403–448.

52 T. A. Daly, M. Wang and S. L. Regen, *Langmuir*, 2011, **27**, 2159–2161.
53 J. Huang and G. W. Feigenson, *Biophys. J.*, 1999, **76**, 2142–2157.
54 F. de Meyer and B. Smit, *Proc. Natl. Acad. Sci. U. S. A.*, 2009, **106**, 3654–3658.
55 T. Róg and M. Pasenkiewicz-Gierula, *FEBS Lett.*, 2001, **502**, 68–71.
56 H. Mizushima, J. Fukasawa and T. Suzuki, *J. Lipid Res.*, 1996, **37**, 361–367.
57 P. Pullmannová, K. Staňková, M. Pospíšilová, B. Školová, J. Zbytovská and K. Vávrová, *Biochim. Biophys. Acta, Biomembr.*, 2014, **1838**, 2115–2126.
58 B. Školová, B. Janůšová, J. Zbytovská, G. Gooris, J. Bouwstra, P. Slepička, P. Berka, J. Roh, K. Palát, A. Hrabálek and K. Vávrová, *Langmuir*, 2013, **29**, 15624–15633.
59 M. Janssens, G. S. Gooris and J. A. Bouwstra, *Biochim. Biophys. Acta, Biomembr.*, 2009, **1788**, 732–742.
60 M. E. Rerek, D. Van Wyck, R. Mendelsohn and D. J. Moore, *Chem. Phys. Lipids*, 2005, **134**, 51–58.
61 D. de Sousa Neto, G. Gooris and J. Bouwstra, *Chem. Phys. Lipids*, 2011, **164**, 184–195.
62 E. H. Mojumdar, Z. Kariman, L. van Kerckhove, G. S. Gooris and J. A. Bouwstra, *Biochim. Biophys. Acta, Biomembr.*, 2014, **1838**, 2473–2483.
63 D. Groen, G. S. Gooris and J. A. Bouwstra, *Biophys. J.*, 2009, **97**, 2242–2249.
64 V. R. Kodati, R. El-Jastimi and M. Lafleur, *J. Phys. Chem.*, 1994, **98**, 12191–12197.
65 C. Das, M. G. Noro and P. D. Olmsted, *Biophys. J.*, 2009, **97**, 1941–1951.

